NURETH14-239

CONTAINMENT COOLER PERFORMANCE IN THE PRESENCE OF LIGHT NON CONDENSABLE GAS WITH COOLER LOCATION AS A PRIMARY PARAMETER

G. Mignot, R. Kapulla, N. Erkan, R. Zboray and D. Paladino

Paul Scherrer Institut, Villigen, Switzerland guillaume.mignot@psi.ch

Abstract

Modeling of steam condensation caused by the operation of a cooler in a containment poses certain challenges. Consequently, the calculated gas flow and the gas distribution in the containment during test scenarios representative of severe accident sequences must be validated against experimental data. Such validation experiments were conducted in the PANDA facility (Switzerland) in the frame of the OECD/SETH-2 project. The performance of the containment cooler was evaluated for two configurations, designated middle and top position, corresponding to the location of the cooler in the containment during a 3-time-phase injection of steam, steamhelium and steam. For the middle position, the results show a deterioration of the cooler performance caused by the accumulation of helium in the cooler-casing which partially blocks the flow path through the cooler. This is followed by a recovery associated with the release of helium from the cooler-casing and the formation of a stable stratified layer on top of the vessel. For the top position a weak degradation of the performance and formation of stable helium rich layer in the center of the vessel was observed.

1. Introduction

Assessing safety issues of LWR containments requires the use of advanced thermal-hydraulics Lumped Parameters codes (LP) and codes with 3D capability (e.g. CFD). The PANDA tests performed in the frame of the OECD/SETH project (Phase 1) had the objective to create an experimental database addressing physical phenomena relevant for LWR containment safety analysis such as the hydrogen stratification build-up [1], [2], [3], and [4]. Analytical activities performed by the project participants aimed in assessing strengths and drawbacks of different codes in analyzing the phenomena encountered in these PANDA tests [5], [6], [7], and [8]. The analytical activities revealed a number of code challenges in relation to: gas transport and stratification build-up for the case of high elevation injection and the prediction of peak gas temperatures.

The experiments under consideration in the present work are designated "containment cooler test series" in the OECD/SETH-2 project. The tests were designed to obtain insight into the dynamic response of a containment cooler during steam and helium injection as well as into its influence on the gas stratification build up and erosion. Up to now the effects of non condensable gas on the heat removal capacity were only studied for quasi steady state conditions, [9] and [10]. Therefore, no transient data are available to characterize the overall cooler performance in a containment-type vessel with changing non condensable gas composition. For the present experiments two large PANDA vessels interconnected by a large bent pipe are used, Figure 1. A cooler was installed in one of the vessels (Vessel 1), and operated during a specific scenario of

steam and helium-steam mixture injection in an environment initially consisting of hot air. Helium is used to simulate hydrogen during the experiments. Past investigations conducted at the THAI facility have shown that gas transport and distribution were well reproduced by substituting hydrogen with helium [11].

The parameters for the entire "containment cooler test series" are: (1) pressurization of the vessels, (2) installed cooler duct (Figure 1-(b)) versus the blockage of this cooler outlet and (3) vertical cooler location in the vessel on the cooler performance. In this paper we will focus on the latter topic. The analysis of the other tests is subject to separate publications.

In the following section, the PANDA facility and its instrumentation are described. This is followed by a discussion of the containment cooler test matrix. The experimental results are presented in terms of helium-steam mixture concentrations as well as density and temperature time plots. To supplement the evolving flow pattern interpretation, locally measured velocity fields are presented.

Some of the axis scales in the figures of the paper are not shown to keep a conservative position with respect to the release of these experimental data. Nevertheless the present overview should allow the reader to follow and understand the main phenomena characterizing the evolution of the experiments.

2. THE PANDA FACILITY

2.1 Description

PANDA is a large-scale thermal-hydraulics test facility designed and used for investigating containment system behaviour and related phenomena for different Advanced Light Water Reactor (ALWR) designs and for large-scale separate effect tests [12].

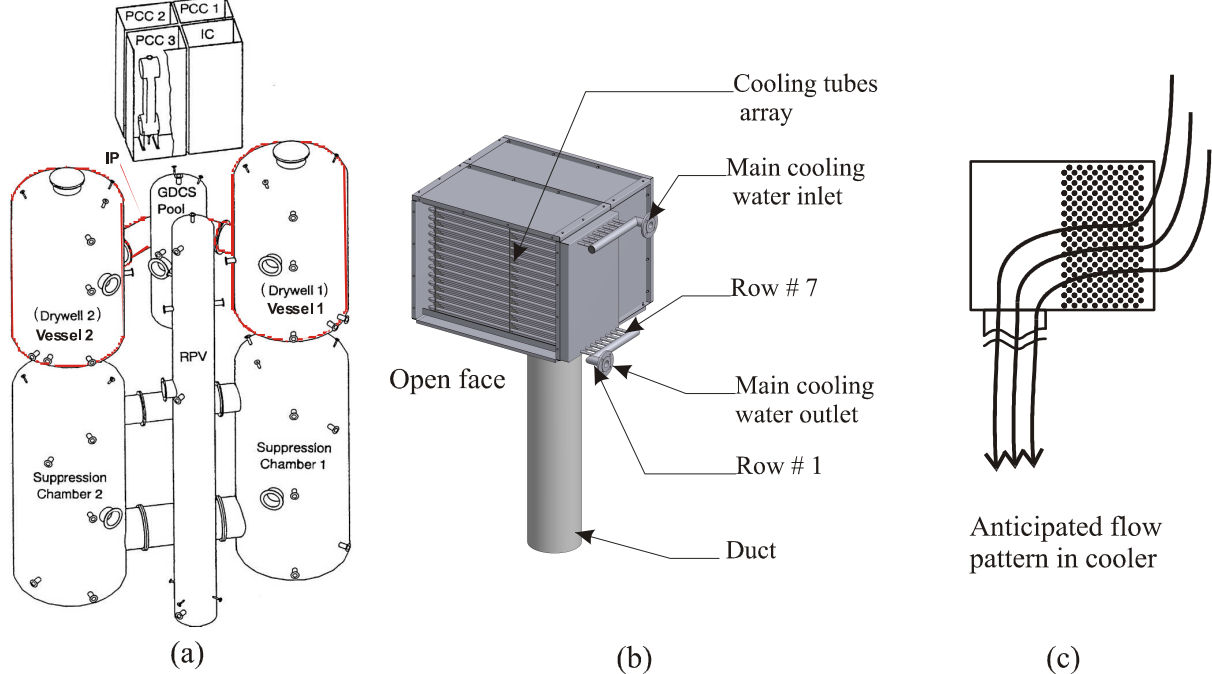


Figure 1: Schematic of the PANDA facility (a), drawing of the main cooler components (b) and anticipated flow in the cooler (c).

The containment compartments and the Reactor Pressure Vessel (RPV) are simulated in PANDA by six cylindrical pressure vessels, Figure 1-(a). The height of the PANDA facility is 25 m, the total volume of the vessels is about 460 m³ and the maximum operating conditions are 10 bar at 200°C. The RPV is electrically heated with a maximum power of 1.5 MW. Various auxiliary systems are available to record and control the initial and boundary conditions of the tests. For the SETH-2 tests, only the RPV and the Drywells parts of the facility are used. In this test series, the experiments are carried out in a large (about 180 m³ total volume) multi-compartment system consisting of two identical vessels connected by a 1 m diameter Interconnecting Pipe (IP). These vessels are referred to as Vessel 1 and Vessel 2 thereafter, Figure 1-(a). Each vessel has a height of 8 m and a diameter of 4 m.

The cooler consists of an 8 tubes in a horizontal staggered serpentine layout enclosed in a casing with a single open face opposite to the interconnecting pipe, Figure 1-(b). In addition, a 1.5 m long duct is installed at the bottom of the cooler to act as an exhaust chimney through which cold gas can leave the cooler, Figure 1-(c). The main cooling water flow is divided in eight sub channels representing the eight columns of the cooler tube array.

2.2 Instrumentation

The PANDA instrumentation allows for the measurement of fluid and wall temperatures, absolute and differential pressures, flow rates, heater power, gas concentrations and flow velocities. The measurement sensors are installed in all facility components, in the system lines and in the auxiliary systems. Compared with OECD/SETH, the measurement grids in Vessel 1 and in Vessel 2 have been refined in SETH-2.

<u>Temperature measurements</u>: Up to 374 K-type thermocouples (TCs) were used for measuring fluid, and inside and outside wall temperatures of Vessel 1, Vessel 2 and the IP (Table 1). An accuracy of around 0.5 °C is assessed. Temperature sensors are installed in the vessels at different heights designated as Level A (near the top of the vessels) to Level T (near the bottom of the vessel) and at different angles and radial distances from the vessel axis.

Table 1: Number of Thermocouples and capillaries installed in Vessel 1, Vessel 2, IP and cooler.

	Thermocouples					
	Fluid	Wall inside	Wall outside	Injection/Vent	•	
Vessel 1	226	23	9	3/3	58	
Vessel 2	58	19	9	0/1	34	
IP	23	3	-	-	15	
Cooler	15	-	2	9/0	11	

<u>Injection and venting flow rates</u>: are measured with vortex flow meters with an accuracy of 1.1 %.

<u>Concentration measurements</u>: Up to 140 sampling lines are installed in the vessels. A maximum of 118 of these samplings lines can be connected to two Mass Spectrometers (MS) for gas concentration measurements. The system can measure any gas concentration and

composition. The gas mixtures used for the SETH-2 tests are either: helium/air, steam/helium or steam/air/helium. The actual number of sampling lines used for measurements varies in each test and during the test evolution. Different scanning sequences are programmed for the MS to monitor facility preconditioning, initial test conditions, and the test evolution. A thermocouple is placed a few millimeters close to each gas sampling port such that gas concentration and temperature measurements are recorded at almost the same spatial location. For steam/air mixtures, an absolute error for the measured steam/air molar fraction of +/- 1.5 % is assessed.

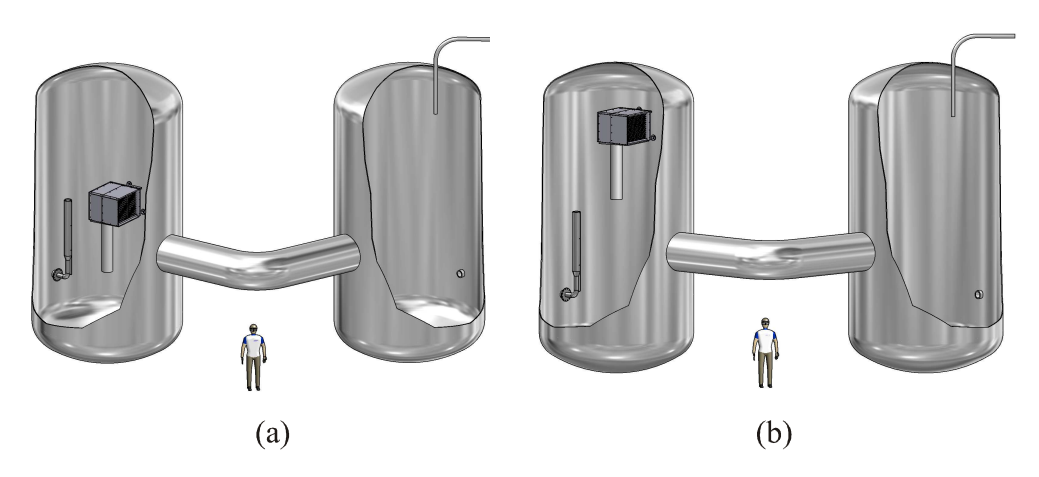
<u>Measurement of 2D velocity fields</u>: A commercial Particle Image Velocimetry (PIV) set-up is used to measure 2D velocity fields in Vessel 1 in a vertical plane aligned with the vertical mid plane of the injection pipe. Olive oil dispersed into small particles by a spray nozzle is used as seeding particles for the PIV technique. The oil particles are injected into the steam flow that is directed into Vessel 1. The PIV system provides 2D instantaneous velocity fields with acquisition rate up to 10 Hz.

3. Test Parameters and Procedure

3.1 Test parameters

A 3-D representation of the compartments used for the two setups that are encountered in the "containment cooler" test series is shown in Figure 2. The experimental series comprises three parameters, (1) the presence or absence of the containment vessel vent (2) the presence or blockage of the cooler duct and (3) the vertical cooler position in the vessel. For both setups the cooler is located in Vessel 1. Two cooler positions have been studied, the *middle* position with the cooler located 100 mm below the injection height, Figure 2 -(a) and the *top* position with the cooler located 2000 mm above the injection, Figure 2 -(b).

The injection is positioned opposite to the interconnecting pipe 500 mm from the wall and 4000 mm from the bottom of the vessel.



(a):configuration for cooler *middle* position (b): configuration for cooler *top* position Figure 2: 3D views of PANDA configuration.

Venting was ensured at the top of Vessel 2 to avoid pressurization of the facility during the test when specified. Finally, the last parameter that was modified in this test series was the presence or not of the duct. The tests parameters for the entire series are presented in Table 2. Test ST4_2 is considered as the reference test since only a single parameter needs to be changed to obtain the configuration of one of the other tests. Only the results from test ST4_2 and ST4_4 will be discussed in the following section.

Table 2: Main parameters for the entire containment cooler series.

Twell 2. Training furthing to the control control control series.						
Test	ST4_1	$ST4_2(_2)^1$	ST4_3	ST4_4		
Venting	no	yes	yes	yes		
Duct Presence	yes	yes	no	yes		
Cooler position ²	middle	middle	middle	top		

3.2 Preconditioning and Test Procedure

Before each test, the facility was preconditioned for a day with pure steam to raise the vessel wall to a temperature sufficient to avoid condensation of the injected steam. Afterwards, the steam was purged from the vessels by injecting hot air from the top of the vessels by mean of blower fans and then pressurized using an air compressor.

Following the preconditioning phase, the water flow in the cooler was started by opening the main cooling water feeding line. After both inlet and outlet cooling water temperatures reached steady state conditions, the experiment was initiated with the injection of superheated steam. The cooler was kept in operation during the entire experiment. The test scenario was divided in three phases. In Phase I, pure steam was injected for about 3600 s, in Phase II, helium was added to the steam injection for about 1800 s upward to the injection outlet. Finally, in Phase III the helium injection was stopped and pure steam was again injected for 3600 s. During the entire test sequence the injected steam flow rate remains constant.

4 Results

Although the measured velocity field will be used to complement the findings deduced from the temperature and concentration signals, the detailed discussion of the velocity field evolution during the test ST4_2_2 and ST4_4 was presented in a previous publication [13] and will not be repeated in the current paper.

4.1 Middle position configuration: Reference Test ST4 2 2

Experiment ST4_2_2 was conducted with no pressurization, with the cooler positioned in the middle (y = 3900 mm) of Vessel 1 and with the presence of the duct, Table 2. In the following section we will explain that and why the actual flow through the cooler is much more complex than the nominal flow pattern anticipated in Figure 1-(c) and that this flow changes considerably during the different phases of the experiment. For this explanation we will use the calculated cooling power, the cooler row outlet temperatures, the helium concentration inside the cooler and

¹ The second extension (2) in the test name refers to a repetition test.

² The *middle* position corresponds to the cooler bottom located a y=3900 mm whereas for the *top* position the bottom cooler is located at y=6000 mm.

in the vessel, the density evolution inside and outside the cooler case as well as two selected averaged velocity fields above the cooler. All these results are presented in Figure 3 where the vertical black lines separate the different phases.

We start our discussion with the calculated cooling power normalized with the latent heat of the injected steam, Figure 3-(a). If all of the injected steam is condensed by the cooler, this results in a normalized cooling power of 1. The two curves represent the integral heat removal considering the temperature difference between the main inlet and outlet of the cooler, black line in Figure 3-(a) and between the inlet of the feeding line (located outside Vessel 1) and the main outlet of the cooler, red line in Figure 3-(a). Consequently, the latter contains also the heat transfer due to condensation on the surface of the water feed line inside the vessel.

During phase I the normalized cooler power continuously increases and reaches almost 1 in the end. This is followed by a continuous decrease of the cooling power down to less than 0.2 through the first part of Phase II. Still in Phase II the cooling power recovers very quickly and results in a maximum of approximately 1.2. Finally, right from the beginning of Phase III (pure steam injection) the cooling power remains almost constant at ≈ 1 .

To explain the cooler performance deterioration during Phase II, as well as the cause for the recovery within Phase II one must take a local perspective. Four out of seven outlet water temperatures are presented in Figure 3-(b). Row # 1 corresponds to the front sub channel (Figure 1-(b)). During Phase I, the outlet temperature difference along the cooling array (#1 to #7) is about 10°C. As soon as Phase II is started (injection of helium and steam) the outlet water temperature of the front row array initially increases slightly whereas the temperatures decrease rapidly for the back rows (#6 and #7) down to 40°C. This decrease in temperature is also observed for the front rows ($\sim t = 4500 \text{ s}$); but later in time. This suggests that the accumulation of helium in the rear part of the cooler (row #7) increasingly hinders the flow passage of steam. This would reduce the condensation rate and, correspondingly, the heat removed by the cooler. This process starts at row #7 and propagates to the front of the cooler. As for the integral power, we see a fast recovery of the heat removal. Finally, during Phase III, the outlet temperature difference is about 45°C between the front (#1) and the back rows (#7), which suggests that the condensation occurs mainly in the first rows of the arrays. During Phase I, the heat released by the condensation process was almost equally divided over the depth of the array whereas in Phase III it is unequally divided over the depth of the cooler tube array leading to an increase for the outlet temperature at the front row and a large decrease for the back row, nonetheless, the overall energy removed being the same, Figure 3-(a).

The normalized helium molar fraction as a function of time inside and outside the cooler is depicted in Figure 3-(c). The sensor locations are presented in Figure 3-(f). The measured helium molar fraction is normalized with the injected helium molar fraction thus an accumulation of helium is indicated by numerical values above 1.

On one hand, we find a continuous helium increase in the upper part of the cooler (CO2 and CO3) and in the upper part of the vessel (A level and H level) during Phase II. On the other hand, no noticeable increase in helium concentration is observed either at the exit of the duct (CO1) or at the bottom of Vessel 1 (T level) suggesting that no fluid flows through the duct.

In the lower part of the cooler array (CO4) as well as in the intermediate vessel level (L level), the helium concentration increases initially before rapidly decreasing to values of around 1 and 0.5, respectively. The time for this sudden change coincides with the time at which the heat-removal recovery was observed. We propose a change in the flow pattern inside the cooler being the cause for this behaviour.

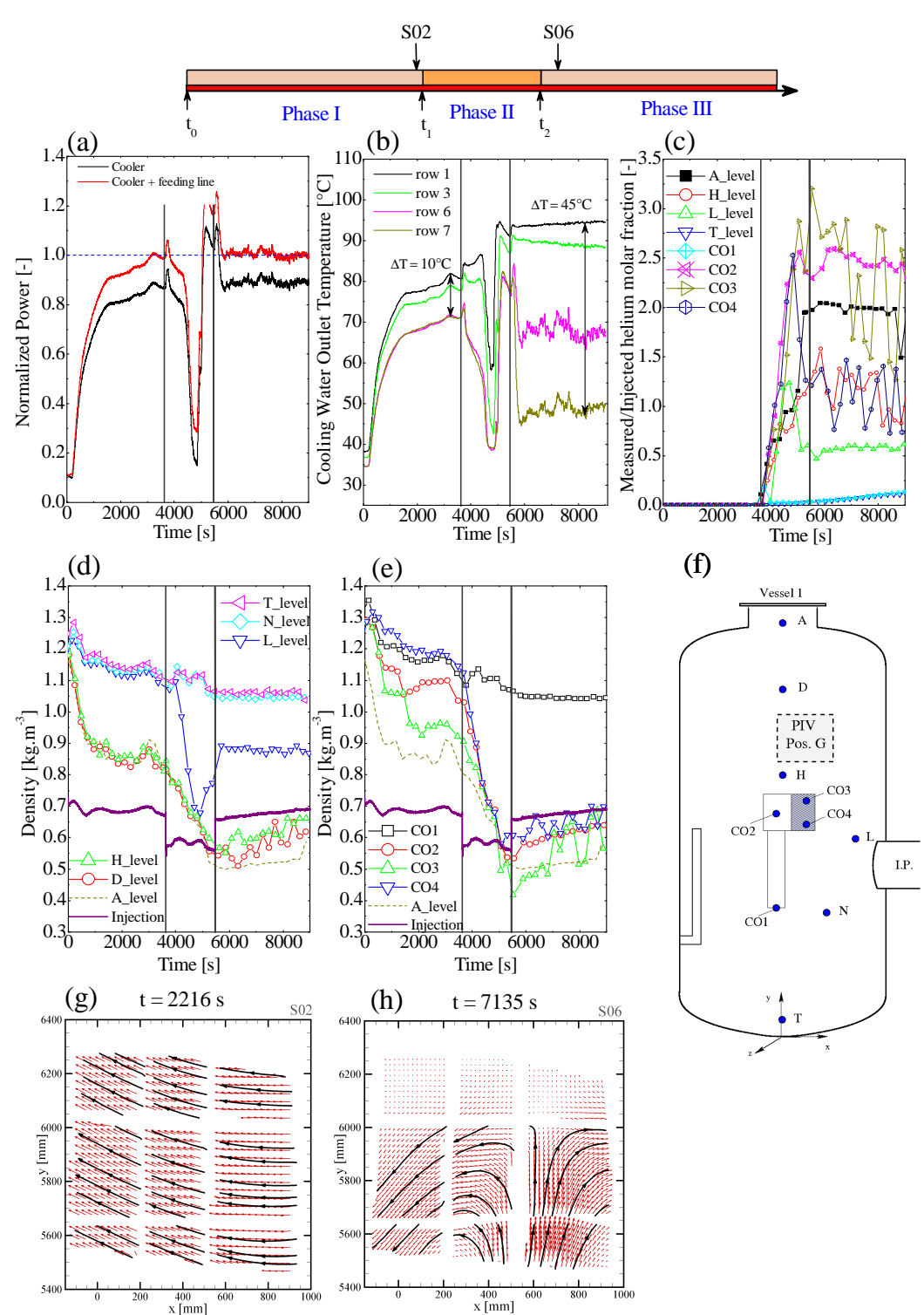


Figure 3: ST4_2_2 results: (a) cooling power, (b) cooling water outlets temperature, (c) helium molar fraction, (d) and (e) gas mixture densities, (f) vessel schematic, (g) and (h) mean velocity fields.

During Phase I, the injected steam mixes with the ambient air through the generation of a large

scale circulation at the top of the vessel induced by the steam injection as depicted in the average velocity field measured in Sequence S02, Figure 3-(g). The velocities show the bottom part of the recirculation loop with an upward movement toward the direction of the injection.

This can be further quantified using the temperature, partial pressure and molar fraction enabling us to calculate the density evolution with ideal gas law at different locations; the results are presented in Figure 3-(d) and Figure 3-(e) for positions inside and outside the cooler, respectively. The densities measured at the top of the facility (A_level) as well as of the injected fluid were plotted as a reference in both figures.

During Phase I, the lighter injected steam rises to the top of the facility resulting in density stratification in the entire vessel. The measurement locations above the cooler (A, D and H level) all show a decrease in density down to ≈0.8 kg·m⁻³ at the end of Phase I whereas the measurement locations below the cooler all show a less pronounced decrease in density down to ≈1.1 kg·m⁻³. During this time, the densities measured in the cooler show values between these two extremes. During phase II the density decreases considerably everywhere above the interconnecting pipe level; including the measurements inside the cooler.

The above discussed accumulation of helium in the cooler (density decreases) overcompensates the effect of lower temperatures (density increases) such that we find the net density decreasing. At $t \approx 4800$ s at locations away from the injection tube and above the interconnecting pipe level the measured density inside and outside the cooler appears quite homogenous, at 0.7 kg·m⁻³. Past $t \approx 4800$ s, the density at the top of the cooler (CO3) reaches values lower than the ones outside and above the cooler. The helium-air-steam mixture accumulated at the top of the cooler has now the potential buoyancy to rise outside the cooler to the top of Vessel 1. At t≈4800 s, the helium rich mixture escapes from the top of the cooler up to level A as justified by the fact that the density of level A reaches value lower than the injection values. This corresponds to the time at which the cooler recovery is observed in the heat removal, Figure 3-(a). In Phase III, the cooler releases a continuous plume of helium rich gas mixture as confirmed by the velocity field. Its density, however, does not reach value low enough to reach the top of the vessel and the plume is therefore confined between the cooler and a low density layer [13]. The averaged velocity field measured in sequence S06 of Phase III, Figure 3-(h), shows the plume head stopped at $y \approx 6000$ mm between level D and H, Figure 3-(f). In the mean time the injected steam jet is also confined between the injection level and an intermediate level as suggested by its density higher than the one above H level. A phenomenon of negatively buoyant jet erosion is expected.

The phenomenology of the flow during the experiment can be distinctly observed using cross sectional temperature map of Vessel 1. Four temperature contour maps with their corresponding schematic view of the expected flow in the cooler are presented in Figure 4. The black crosses in these contour maps represent temperature measurement locations and the temperature scale increases from blue to red; a linear interpolation between the closest neighbouring points was calculated to obtain the contour representation.

During Phase I, superheated steam is filling the top of the vessel, Figure 4-(a). The condensation occurring in the cooler creates a suction effect, which is further enhanced by the presence of the downward chimney. The cold temperature measured at the exit of the duct proves the presence of flow through the duct. The temperature gradient, gray circle in Figure 4-(a), associated with the steam concentration gradient suggests that the steam mixture remains confined above the cooler level. During Phase I, the flow passes most probably through the entire depth of the cooler tube array (Figure 1-(c)) as confirmed by the small outlet temperature differences (Figure 3-(b)) and exit through the duct.

The temperature map which corresponds to the beginning of Phase II, when deterioration of the heat removal occurs, is presented in Figure 4-(b). The duct outlet temperature is now similar to its surrounding. Thus it is concluded, that the accumulation of helium discussed previously, has lead to a partially blockage of the flow passage such that the flow through the duct has stopped. The steam/air /helium mixture flowing through the cooler cannot penetrate the entire depth of the array due to the resistance of a helium rich mixture confined in the casing Figure 4-(b). This explains the deterioration of the heat removal beginning from the back end of the array. The cooled gas mixture exits the cooler through the bottom part of the cooler open side, which explains the rapid drop in density observed at L level, Figure 3-(d). The accumulation of helium during Phase II ($t \approx 4800 \text{ s}$) is probably such strong that almost no flow can pass through the cooler array; this corresponds to the minimum heat removal observed in Figure 3-(a).

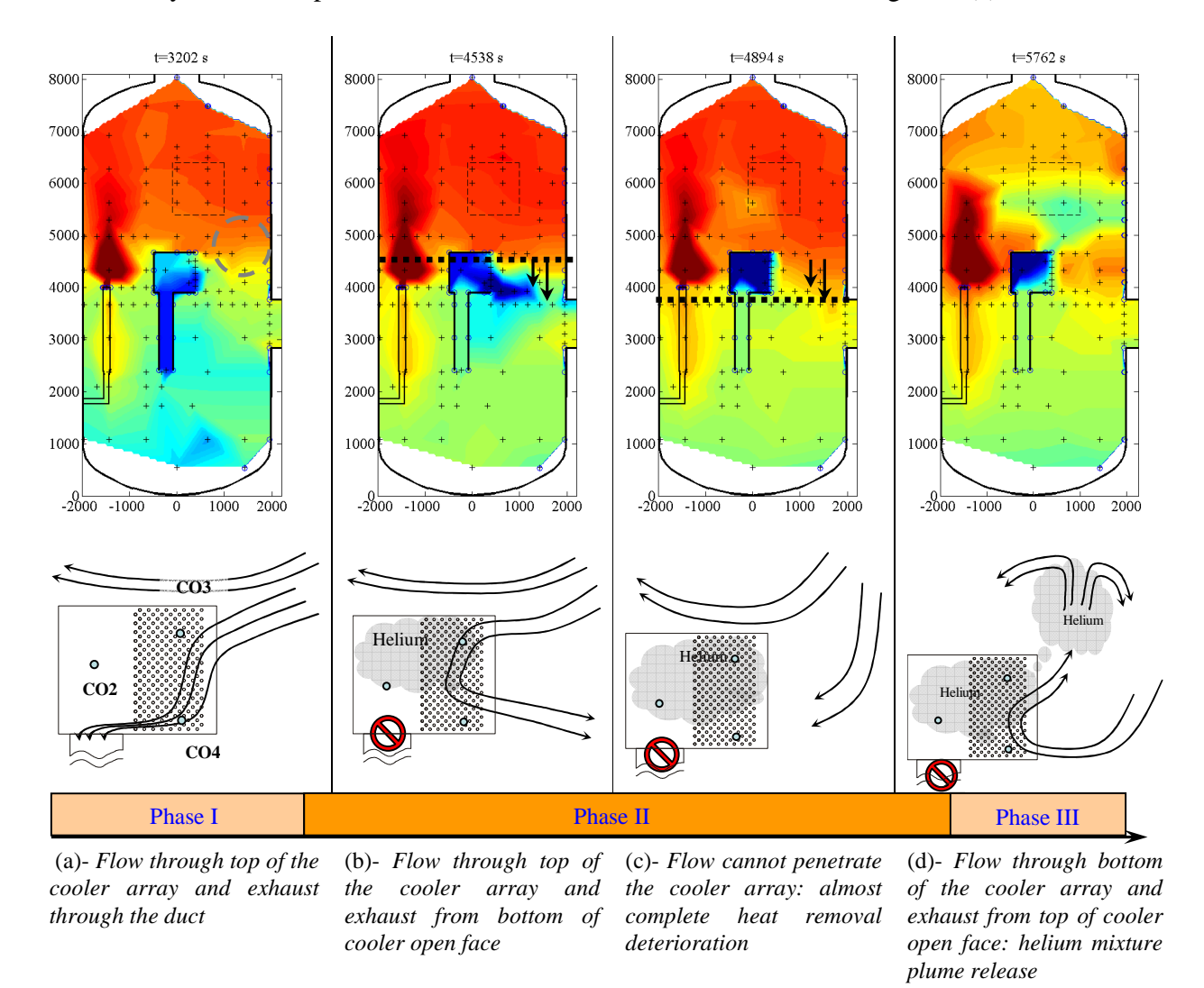


Figure 4: ST4_2_2 phenomenology description.

During Phase II, the hot helium/steam rich mixture accumulates at the top of the vessel and the interface towards the helium/steam poor mixture in the lower part of the vessel moves

continuously downwards up to a level below the cooler inlet, represented with black arrows and dash line in Figure 4-(b) and Figure 4-(c). The heat removal recovery observed at the end of Phase II can be explained by the fact that the helium/steam mixture outside the cooler finds its way finally through the bottom of the cooler tube array, Figure 4-(d), which increases the condensation rate again. The break up of an unstable density stratification between the inside and outside part of the cooler, seems to trigger the cooler recovery phase. The heavier hot gas mixture outside the cooler might have pushed the lighter colder helium rich mixture out of the cooler case creating a new flow circulation pattern in the tube array. However, this flow pattern in the cooler is confined to the first few cooler rods at the front of the tube array as discussed previously in the context of the row temperatures, Figure 3-(b).

Finally, the double confined jet/plume situation of phase III is depicted in Figure 4-(d) with a hot steam (dark red) confined jet next to the wall above the injection tube on the left and a colder helium rich plume (blue green) above the cooler casing on the right. Note that the temperature interface corresponds to the front end of the plume observed also in the velocity field, Figure 3-(h).

4.2 Top position configuration: Test ST4_4

The way of presenting the results for experiment ST4_4 (Figure 5 and Figure 6) correspond to those for ST4_2_2. For experiment ST4_4 the cooler is located close to the top of the vessel, 2100 mm higher than for ST4_2_2.

Although present for experiment ST4 4, the cooler heat removal deterioration during Phase II does not appear as strong as previously observed for ST4 2 2, Figure 5-(a). The presence of helium in the injected fluid in Phase II decreases the condensation rate in the cooler and correspondingly the heat removal capacity of the cooler. During Phase I, the outlet temperatures of the rows show a difference of ≈14°C through the depth of the array, Figure 5-(b) again indicating that more steam condenses at the inlet of cooler compared with the rear part. This temperature difference increases slightly during Phase II to ≈25°C and returns slowly to its value observed at the end of phase I as the helium injection is stopped in Phase III. The slower temperature decay compared to ST4 2 2, can be associated with the slower build-up of the helium accumulation in the cooler, Figure 5-(c). The measured injected helium molar fraction ratio reaches only a value of 2 at the end of Phase II for the CO2 sensor compared to the 2.5 for experiment ST4_2_2. The helium content, however, starts decaying as soon as the helium injection is stopped. In fact, one of the main differences between the two experiments is the actual flow through the duct. Whereas the flow stopped for ST4_2_2, the gas mixture released by the back of the cooler array, keeps continuously flowing and is even enhanced during Phase II of experiment ST4_4 (Figure 6-(b) versus Figure 4-(b)). Consequently, helium is transported through the duct towards the lower part of the vessel. This is confirmed by the helium concentration measurement at location CO1 which follows the trend at location CO2, Figure 5-(c). The helium is mixed with the gas below the cooler which explains the rapid increase in helium concentration at M and T level at t \approx 7000 s and t \approx 8000 s, Figure 5-(c). In addition to the duct outlet flow, vertical downward velocities have been measured below the cooler open face, Figure 5-(g), suggesting that part of the cooled gas is also escaping the cooler casing from the bottom of the open face, Figure 6-(a). The density outside the cooler is always higher than the density of the gas injected through the tube, which is in contrast to experiment ST4_2_2. This emphasizes the potential of the jet to reach the top of the facility during the entire test sequence.

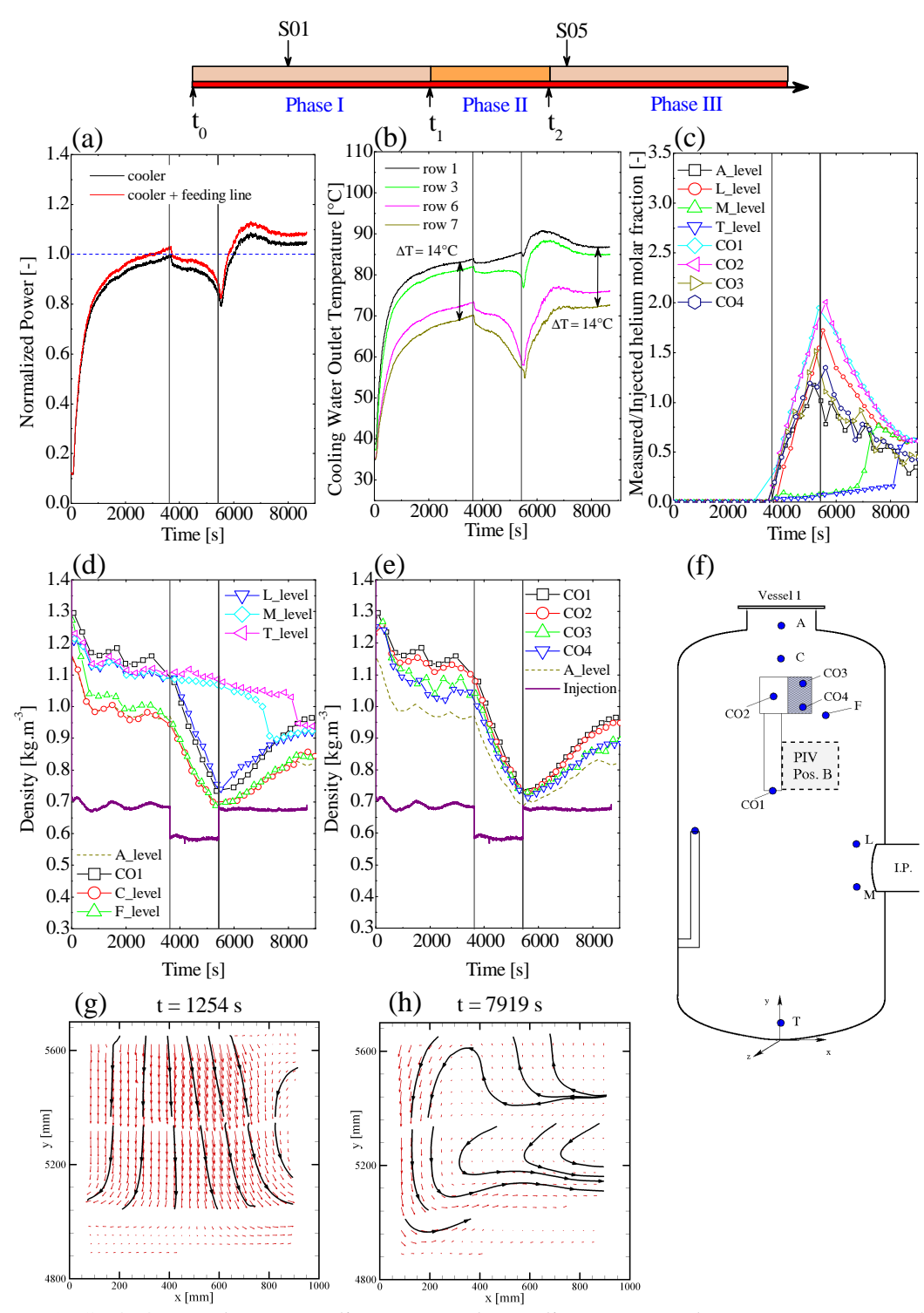


Figure 5 : ST4_4_Results: (a) cooling power, (b) cooling water outlets temperature, (c) helium molar fraction, (d) and (e) gas mixture densities, (f) vessel schematic, (g) and (h) mean velocity fields.

Mixing is therefore always ensured at the top of the facility and no strong density stratification is observed above L level, Figure 5-(d). This statement holds also true for the densities inside the cooler. All four densities, CO1, CO2, CO3 and CO4, show a similar trend, Figure 5-(e), with almost identical values during Phase II.

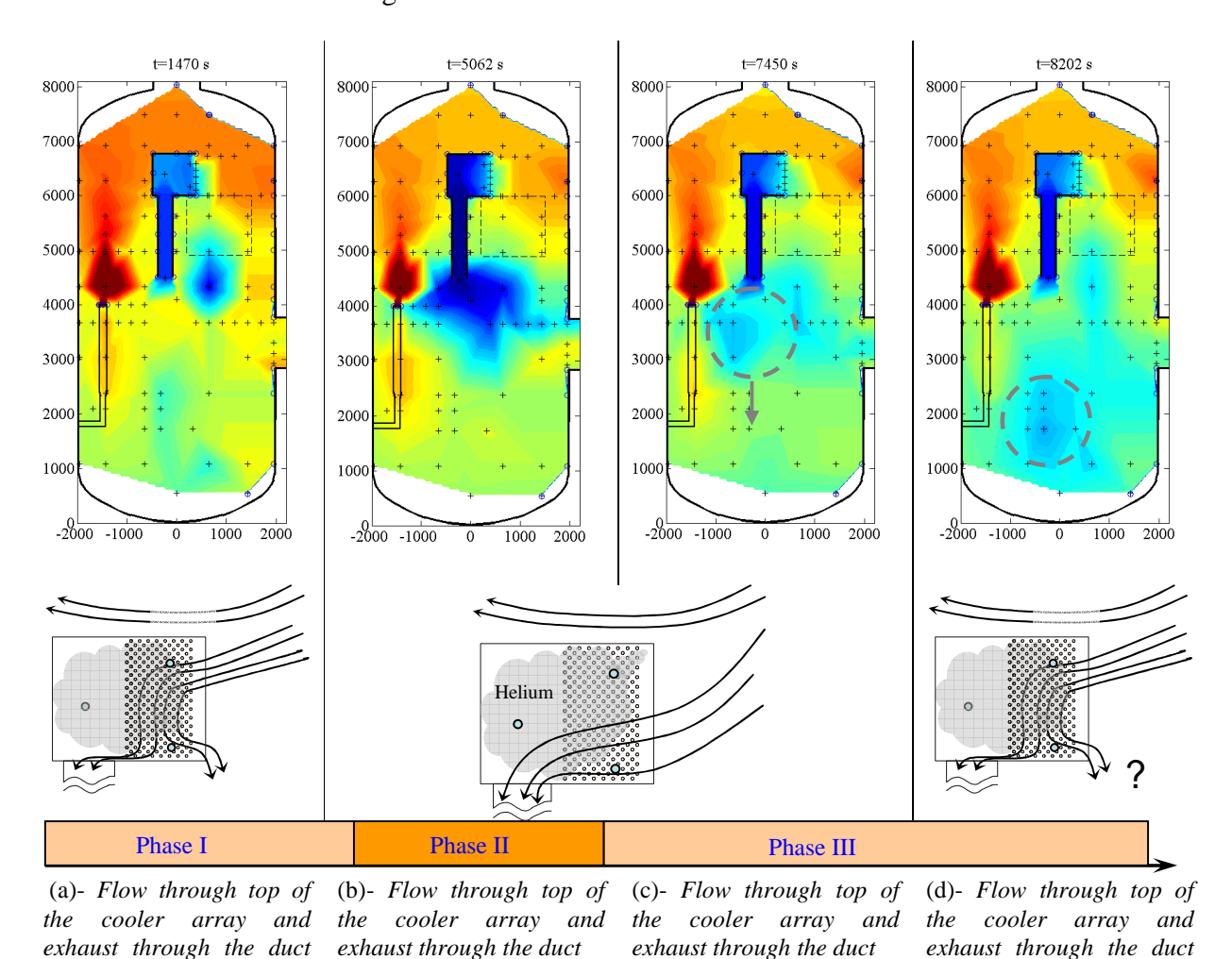


Figure 6: ST4_4 Phenomenology description.

and bottom front of the

cooler?

and bottom front of the

cooler

The sole density stratification is located between L and M level at the end of Phase II ($t \approx 5400 \text{ s}$) with a density difference of 0.35 kg.m⁻³. The similar behaviour of the densities measured at CO1 and L locations suggest that the gas mixture outflow remains confined below the duct at an intermediated level above the M level. This is also supported by temperature measurements showing a pocket of colder fluid for 3500 mm < y < 5000 mm, Figure 6–(b). As the helium injection is stopped for Phase III; the duct outflow gas density (CO1) increases slowly thus pushing down the colder helium rich pocket while mixing with the fluid confined below. One can observe this phenomenon in Figure 6-(c) and -(d) marked with the gray dash circle. The downward movement of the pocket is also confirmed by the density and helium concentration measurement at t $\approx 7000 \text{ s}$ for M level and at t $\approx 8000 \text{ s}$ for T level. Additionally in Phase III,

also the velocity vector field changes dramatically from a downwards flow (Phase I) to a natural convection loop activated by the presence of the cold duct at $x \approx 0$ mm and the warmer fluid closer to the vessel wall $x \ge 1500$ mm.

5 Conclusions

Experiments with an operating containment cooler interacting with a vertical wall jet composed successively of pure steam (Phase I), a steam/helium mixture (Phase II) and finally again pure steam (Phase III) were conducted in the PANDA facility. The cooler performance during the different phases of the experiment as well as the overall flow patterns within the vessel containing the cooler was addressed for two configurations, *middle* and *top*, referring to the location of the cooler in the vessel.

For both configurations, the pure steam injection during Phase I lead with a transient process to an equilibrium where the heat injected through the jet was balanced by the heat removal of the cooler.

For the *middle* configuration, a strong degradation of the cooler performance down to 20 % was observed during the injection of a helium/steam mixture in Phase II, which was caused by an accumulation of helium rich gas stratification inside the cooler. The helium rich gas accumulation blocked the flow through the exhaust duct. Still during Phase II, the cooler performance recovers; despite the fact that the duct flow remains blocked for the rest of the test. The recovery was associated with a continuous release of helium rich gas mixture from the cooler that lead to the formation of strong density stratification on top of the vessel. In Phase III, neither the injected steam jet nor the escaping helium gas mixture plume was able to penetrate the stratified layer, which remains stable for the rest of the test.

For the *top* configuration, in Phase II, an accumulation of helium was also observed in the cooler casing but to a smaller extent compared to the *middle* configuration, such that the performance degradation remained limited. Additionally, the flow through the duct was enhanced leading to the formation of a helium rich gas mixture accumulation at the middle elevation of the vessel. The presence of the cooler in the upper part of the vessel enhanced the mixing such that density stratification, weaker than for the middle configuration, was observed only in the lower part of the vessel. This stratified layer was eroded before the end of Phase III.

In summary the *top* configuration allows for better performance of the cooler in presence of light non condensable gas and a better overall mixing than the *middle* configuration.

Acknowledgments

The authors gratefully acknowledge the support of all of the countries and international organizations participating in the OECD/SETH-2 project as well as the members of the Management Board and the Program Review Group of the SETH-2 project. In particular we would like to thank the staff members Max Fehlmann, Chantal Wellauer and Wilhelm-Martin Bissels for their engaged support in conducting these experiments.

References

[1] O. Auban, R. Zboray and D. Paladino, "Investigation of large-scale gas mixing and stratification phenomena related to LWR containment studies in the PANDA facility", *Nuclear Engineering and Design*, Vol. 237, pp. 409-419 (2007).

- [2] R. Zboray and D. Paladino, "Experiments on basic thermal-hydraulic phenomena relevant for LWR containment: Gas mixing and transport induced by buoyant jets in a multi-compartment geometry", *Nuclear Engineering and Design*, Vol. 240, pp. 3158-3169 (2010).
- [3] D. Paladino, M. Andreani, R. Zboray and J. Dreier, "Flow transport and mixing induced by Horizontal jet impinging on a vertical wall of the multi-compartment PANDA facility", *Nuclear Engineering and Design*, Vol. 240, pp. 2054-2065 (2010).
- [4] D. Paladino, R. Zboray, P. Benz, M. Andreani, "Three gas-mixture plume inducing mixing and stratification in a multi-compartment containment", *Nuclear Engineering and Design*, Vol. 240, pp. 210-220 (2010).
- [5] "OECD/SETH Seminar 2007", Institut de Radioprotection et de Sûreté Nucléaire, Fontenay-Aux-Roses cedex, France, June 18-19, 2007.
- [6] P. Royl, J. R. Travis, W. Breitung, "GASFLOW Validation with Steam/Helium Distribution in a Multi Room Test Facility (PANDA SETH test 25), <u>Proceeding of the Annual Meeting on nuclear Technology</u>, Hamburg, Germany May 27-29, 2008.
- [7] M. Andreani, D. Paladino, T. George, "Simulation of basic gas mixing tests with condensation in the PANDA facility using the GOTHIC code", *Nuclear Engineering and Design*, Vol. 240, pp. 1528-1547 (2010).
- [8] M. Andreani, D. Paladino, "Simulation of gas mixing and Transport in a multicompartment geometry using the GOTHIC containment code and relatively coarse meshes", Nuclear Engineering and Design, 240 (2010) 1506-1527
- [9] S. Yokobori, T. Tobimatsu, M. Akinaga, M. Fukasawa and H. Nagasaka, "Containment vessel cooling test by BWR drywell cooler under severe accident conditions", *Transaction of the Japan Atomic Energy Society*, **2**, 3, 230-239 (2003).
- [10] H. Nagasaka, T. Tobimatsu, M. Tahara, S. Yokobori and M. Akinaga, "System transient tests with a BWR dry well cooler used as a countermeasure in severe accidents", *Transaction of the Japan Atomic Energy Society*, **2**, 3, 240-250 (2003).
- [11] OECD/CSNI, "OECD/THAI Project, hydrogen and fission product issues relevant for containment safety assessment under sever accident conditions", Nuclear Energy Agency, Committee on the safety of nuclear installations, NEA/CSNI/R(2010)3, JT03285992.
- [12] J. Dreier, D. Paladino, M. Huggenberger, M. Andreani, G. Yadigaroglu, 2008. PANDA: a Large Scale Multi-Purpose, Test Facility for LWR Safety Research, <u>Proceedings of the International Conference on the Physics of Reactors (PHYSOR08)</u>, Interlaken, Switzerland.
- [13] R. Kapulla, G. Mignot, N. Erkan, R.Zboray and D. Paladino, "Thermal hydraulic phenomena caused by the interaction of steam and steam-helium mixture wall jets with a containment cooler", <u>Proceeding of the International Congress on Advances in Power Plants (ICAPP 11)</u>- Nice, France- May 2011.